

## AFM tip characterization by Kelvin probe force microscopy

C Barth<sup>1,5</sup>, T Hynninen<sup>3,4</sup>, M Bielecki<sup>2</sup>, C R Henry<sup>1</sup>,  
A S Foster<sup>3,4</sup>, F Esch<sup>2</sup> and U Heiz<sup>2</sup>

<sup>1</sup> Centre Interdisciplinaire de Nanoscience de Marseille (CINaM<sup>6</sup> UPR 3118), CNRS, Campus de Luminy, Case 913, 13288 Marseille Cedex 09, France

<sup>2</sup> Lehrstuhl für Physikalische Chemie, Technische Universität München, Department Chemie, Lichtenbergstr 4, D-85748 Garching, Germany

<sup>3</sup> Department of Physics, Tampere University of Technology, PO Box 692, FIN-33101 Tampere, Finland

<sup>4</sup> Department of Applied Physics, Aalto University School of Science and Technology, PO Box 11100, FI-00076 Helsinki, Finland

E-mail: [barth@cinam.univ-mrs.fr](mailto:barth@cinam.univ-mrs.fr)

*New Journal of Physics* **12** (2010) 093024 (14pp)


Received 2 July 2010

Published 15 September 2010

Online at <http://www.njp.org/>

doi:10.1088/1367-2630/12/9/093024

**Abstract.** Reliable determination of the surface potential with spatial resolution is key for understanding complex interfaces that range from nanostructured surfaces to molecular systems to biological membranes. In this context, Kelvin probe force microscopy (KPFM) has become the atomic force microscope (AFM) method of choice for mapping the local electrostatic surface potential as it changes laterally due to variations in the surface work function or surface charge distribution. For reliable KPFM measurements, the influence of the tip on the measured electrostatic surface potential has to be understood. We show here that the mean Kelvin voltage can be used for a straightforward characterization of the electrostatic signature of neutral, charged and polar tips, the starting point for quantitative measurements and for tip-charge control for AFM manipulation experiments. This is proven on thin MgO(001) islands supported on Ag(001) and is supported by theoretical modeling, which shows that single ions or dipoles at the tip apex dominate the mean Kelvin voltage.

 Online supplementary data available from [stacks.iop.org/NJP/12/093024/mmedia](http://stacks.iop.org/NJP/12/093024/mmedia)

<sup>5</sup> Author to whom any correspondence should be addressed.

<sup>6</sup> The CINaM is associated with the Aix-Marseille university.

## Contents

<b>1. Introduction</b>	<b>2</b>
<b>2. Methods</b>	<b>3</b>
<b>3. Results</b>	<b>3</b>
<b>4. Discussion</b>	<b>9</b>
<b>5. Conclusion and perspectives</b>	<b>11</b>
<b>Acknowledgments</b>	<b>12</b>
<b>References</b>	<b>12</b>

## 1. Introduction

Since its introduction by Lord Kelvin in 1898 [1], the *classical* Kelvin probe technique [2] has been used for precise work function measurements in surface physics [3] and surface chemistry [4, 5]. Following the invention of the atomic force microscope (AFM) in 1986 [6], Kelvin probe techniques became *local*, offering resolution at the nanometer scale. The development of electrostatic AFMs for the study of work function and charge-related phenomena on surfaces [7] has led to Kelvin probe force microscopy (KPFM) [8, 9] becoming a well-established surface science tool in many scientific disciplines [10, 11].

On clean surfaces, work function measurements in the meV range with a high lateral resolution have so far been best realized by KPFM if the AFM is used in the noncontact mode (nc-AFM) [12] and in ultrahigh vacuum (UHV) [13, 14]. The surfaces of metals, semiconductors [15] and thin insulating films supported on metal surfaces [16]–[18] can be measured regardless of the presence of supported metal nanoclusters [19] or molecules [20]. The lateral resolution depends on the dimensions of the tip-apex and the objects supported on the surface [18, 21], and in some cases an atomic scale contrast can be observed [22]. Not only work function changes but also the charge distribution on insulator surfaces [23, 24] and their influence on nano-objects, such as metal nanoclusters [25, 26], can be precisely measured with this technique. The sensitivity of the Kelvin microscope is sufficiently high that even surface charges below the equivalent charge of one electron can be detected [24, 27, 28].

The electrostatic signature of the tip as the sensing probe in KPFM offers a possible route to AFM tip characterization—a connection that has never been investigated systematically up to now. The idea is to use KPFM for characterization of the electrostatic potential of the tip as it is influenced by fixed charges or dipoles, which get accidentally adsorbed at the tip apex during imaging or can be attached at will by functionalization [29]. Changes in the topographical contrast are especially expected on structured surfaces, where the charge or dipole distribution changes locally. For this purpose, a clean Ag(001) substrate was prepared, onto which thin MgO(001) islands were grown, breaking the symmetry of the electrostatic tip–silver interaction due to its strong dipole. It is shown that the mean Kelvin signal changes from negative to positive values when the tip changes its potential from negative to positive upon tip-changes and vice versa. The tip potential could be identified with the help of the topography contrast, as shown recently [18]. The influence of the tip potential on the Kelvin voltage can even be quantified: a simple model of the electrostatic tip–surface interaction shows how charges or dipoles corresponding to single ions or molecules at the tip change the Kelvin voltage.

## 2. Methods

Frequency-modulated nc-AFM and KPFM experiments were performed in the low  $10^{-10}$  mbar pressure range and at room temperature with a VT Omicron AFM/STM. A conducting silicon cantilever (Nanosensors, p-Si,  $0.015 \Omega \text{ cm}$ , 318 kHz resonance frequency and  $29 \text{ N m}^{-1}$  spring constant) was used. KPFM measurements were performed in the frequency modulation mode [14, 23], where a dc ( $U_{\text{dc}}$ ) and an ac ( $U_{\text{ac}}$ ) voltage with frequency  $f_{\text{ac}}$  were applied between the tip and the surface (tip at ground). In a KPFM measurement, the electrostatic tip–surface interaction is minimized at each point on the surface by the dc Kelvin voltage, which yields the contact potential difference (CPD) between the tip and the surface  $U_{\text{dc, min}} = -U_{\text{CPD}} = -(\phi_{\text{sample}} - \phi_{\text{tip}})/e$  for a neutral tip. The Kelvin modulation is applied in the constant  $\Delta f$  mode of the nc-AFM (topography imaging mode), so that a topography and a Kelvin image are obtained at the same time in a single measurement. Although the tips carried a thin native oxide layer, a well-defined CPD between the tip and the surface could be measured, which differed only by an offset in comparison to metallic tips [30]. All images were acquired in the constant detuning mode with the Omicron Matrix system and prepared with Gwyddion software.

The silver surface of a single crystal (Surface Preparation Lab—Holland, 99.999%, polished surface with  $0.1^\circ$  precision) was prepared by several cycles of ion sputtering (1.0 keV, 40 min) and annealing ( $550^\circ \text{C}$ , 30 min) followed by slow cooling ( $10 \text{ K min}^{-1}$ ) for optimizing terrace widths. A thin MgO(001) film was then grown by evaporating Mg from a hot magnesium ribbon band ( $\sim 0.1 \text{ ML min}^{-1}$ ) in an oxygen atmosphere ( $1 \times 10^{-6}$  mbar) onto the silver surface ( $300^\circ \text{C}$ ).

Atomistic simulations were carried out using the SciFi AFM simulation tool [31, 32]. Various MgO tips from single ions to clusters of 64 atoms were considered. The conducting macrotip and sample were treated as continuous media with their contribution analyzed using the image charge scheme. The Kelvin voltage was then determined from the calculated force versus voltage in the same way as the other models (see supporting information).

## 3. Results

Typical tip-changes during imaging of the topography are shown in the topography (a) and Kelvin image (b) in figure 1. The measurement was performed on a silver surface, onto which an MgO film with a nominal thickness of 0.3 ML was grown. Two types of MgO islands exist for this specific MgO coverage [33, 34]: one type of MgO island is supported on the silver surface, whereas the other one is partially embedded into the surface (i.e. supported on the second silver layer). In the following, the two types of islands are called  $\text{MgO}_a$  (embedded) and  $\text{MgO}_b$  (supported) islands. Calculations and STM measurements indicate that the  $\text{MgO}_a$  and  $\text{MgO}_b$  islands have a height of  $\sim 0.5 \text{ \AA}$  [18, 34] and  $\sim 2.4 \text{ \AA}$  [18, 34, 35], respectively, with respect to the top silver layer.

Five tip-changes (tip changes I–V) can be seen in the topography image (a) dividing the image into three large regions (regions I–III). The topography contrast helps us to identify the electrostatic potential of the tip as follows [18]: when the scanning was started (region I, scanning was performed from the bottom to the top), both types of MgO(001) islands were imaged as dark islands corresponding to apparent depressions ( $\Delta z_{\text{MgO}-a} = -3.1 \text{ \AA}$  and  $\Delta z_{\text{MgO}-b} = -1.2 \text{ \AA}$ ). Such a dark contrast does not represent the true topography of the

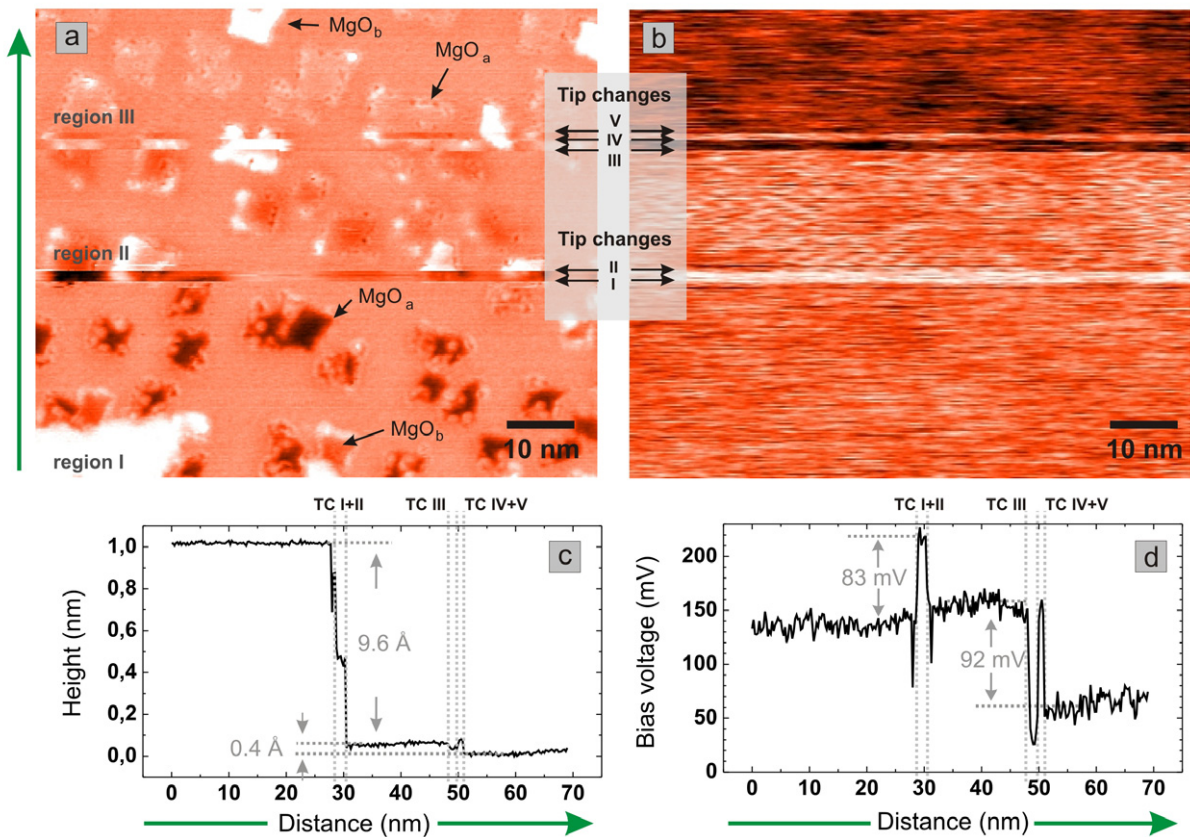


**Figure 1.** Topography (a) and raw Kelvin image (b) obtained within one measurement. The green arrows point in the slow scanning direction. For clarity, a mean subtraction routine and a subsequent plane fit were applied on the topography image to show all details in high contrast. Contrast of the MgO islands with respect to the surrounding clean Ag surface:  $\Delta z_{\text{MgO}-a} = -3.1 \text{ \AA}$  and  $\Delta z_{\text{MgO}-b} = -1.2 \text{ \AA}$  (region I),  $\Delta z_{\text{MgO}} \approx -4.5 \text{ \AA}$  (TC I and TC II),  $\Delta z_{\text{MgO}-a} = -0.4 \text{ \AA}$  and  $\Delta z_{\text{MgO}-b} = +1.7 \text{ \AA}$  (region II),  $\Delta z_{\text{MgO}-a} \approx +1.3 \text{ \AA}$  and  $\Delta z_{\text{MgO}-b} \approx +3.0 \text{ \AA}$  (TC III and TC IV),  $\Delta z_{\text{MgO}-b} = +2.2 \text{ \AA}$  and  $\Delta z_{\text{MgO}-a} = +0.3 \text{ \AA}$  (region III). (c) Averaged profile taken from the raw topography image along the slow scanning direction. (d) The same type of averaged profile from the Kelvin image.  $83 \times 69 \text{ nm}^2$ ,  $\Delta f = -30 \text{ Hz}$ ,  $v_{\text{Scan}} = 0.5 \text{ Hz}$ ,  $U_{\text{ac}} = 0.3 \text{ V}$ ,  $f_{\text{ac}} = 630 \text{ Hz}$ .

protruding MgO islands but is instead a result of a tip effect: tips with a net positive potential at the apex (*positive tips*) encounter a repulsive interaction with the MgO islands, which have a net positive surface charge due to their dipole moment pointing out of the surface [35]. Since such images are obtained in the constant  $\Delta f$  mode of the nc-AFM, the tip approaches the MgO islands during scanning, until the attractive van der Waals contribution outbalances the repulsion and the initial detuning  $\Delta f$  is recovered—the islands appear as dark islands in the images.

After the imaging of surface region I, a tip-change appeared and the islands became darker within six scanning lines—in the line of our observation before, the tip got thus even more positively charged for a short time. Upon tip-change II, the MgO<sub>a</sub> islands appeared less dark,

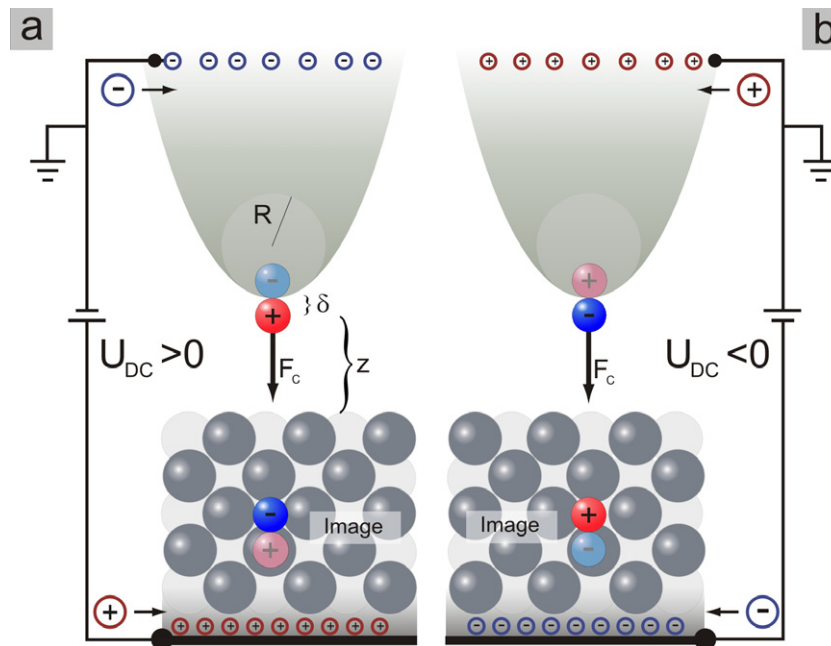


**Figure 2.** The tip–surface interaction in KPFM when the tip-apex carries ions or dipoles (shaded). (a) A positive tip induces negative image charges in the metal substrate, which leads to a long-range electrostatic force. The electrostatic force is balanced through the Kelvin loop by a positive bias voltage (positive charges in the sample and negative charges in the tip). (b) The same principle for a negative tip, but with an inverted potential difference between the tip and the surface.

whereas the  $\text{MgO}_b$  islands became bright—a less positive but somewhat stable tip was thus imaging this part of the surface (region II). After tip-change III, the tip imaged all islands as bright islands for a short time (six scanning lines). A positive tip after tip-change IV then imaged the islands as dark islands, again within a short time (four scanning lines). Tip-change V led finally to a tip that was stable until the end of the image: the tip imaged the  $\text{MgO}$  islands as bright islands with correct height values of the supported and embedded islands on  $\text{Ag}(001)$  ( $\Delta z_{\text{MgO}-b} = +2.2 \text{ \AA}$  and  $\Delta z_{\text{MgO}-a} = +0.3 \text{ \AA}$ ) [18, 34]. This latter, stable tip can be assigned to a *neutral tip*, which was probably composed of stoichiometric uncharged material. Such tips are known to reproduce the correct topography of the surface accurately [18].

In principle, the Kelvin microscope is quite sensitive to variations in the electrostatic surface potential, which are induced by single surface charges with an equivalent charge of one electron or less [24, 28]. Due to symmetry reasons, the same sensitivity should be found for the case that it is the tip that carries the charge and not the surface. In other words, tip-changes where the tip becomes occasionally positive or negative should, in principle, be detectable by KPFM. Indeed, an unequivocal correlation between the tip-changes in the topography and changes in the Kelvin image can be observed (figure 1): the mean Kelvin signal changed at exactly the same time when the tip changed.

To understand this contrast, the electrostatic tip–surface interaction must be analyzed. A positive tip with a positive charge or dipole at its apex, for instance, polarizes the silver substrate (figure 2(a)). In the picture of ‘image charges’, this means that the charge or dipole



produces an image charge or dipole of opposite sign, located below the silver surface at a relatively large distance ( $2\times$  the tip–surface distance). This electrostatic interaction is thus of long-range character and the whole substrate is polarized, regardless of the presence of MgO islands. When the Kelvin mode of the microscope is active, the electrostatic force between the tip charge and its image charge is balanced by an opposite electrostatic field induced by the dc voltage of the Kelvin setup. For balancing the electrostatic field induced by a positive charge or dipole at the tip, for example, the positive charge must be brought onto the sample. This is done by applying a positive sample voltage, as shown in figure 2(a) (the tip is at the ground, as in the experiment). This is in agreement with the positive Kelvin voltage of +135 mV, which was applied during imaging of surface region I (figure 1(d)). After tip-change I, the tip became more positive for a short time and, indeed, the bias voltage applied at the sample was also more positive (+215 mV). After a similar voltage was applied in region II (+157 mV) with respect to region I, the voltage dropped briefly to +26 mV but increased to +157 mV right after tip-change IV, which is again in agreement with that a positive tip imaged the surface within a couple of scanning lines. After tip-change V, the voltage remained at a constant value of +66 mV in region III.

For a deeper understanding of the mean Kelvin voltage, a simple model based on image charges can be considered where a charge  $q$  is attached to a spherical, conductive tip (see supporting information). The total electrostatic energy is the sum of the Coulomb interaction between the charge and its image charges in the substrate and tip, and the capacity built up by the tip and the surface. The Kelvin voltage can then be described as

$$U_{\text{dc},\text{min}} = \frac{q \delta}{\pi \varepsilon R^2} \frac{(1 + z/R)^2}{(1 + 2z/R) \cdot (z/R)} - U_{\text{CPD}}. \quad (1)$$

The parameters  $R$ ,  $z$ ,  $U_{\text{CPD}}$  and  $\varepsilon$  denote the radius of the sphere, the tip–surface distance, the CPD between the tip and the surface and the dielectric constant, respectively. The distance  $\delta$  is the distance between the charge and the sphere. A similar expression is obtained for a dipole with moment  $p$ , which polarizes the metal plane and the tip,

$$U_{\text{dc},\text{min}} = \frac{p \cos(\theta)}{\pi \varepsilon R^2} \frac{(1 + z/R)^2}{(1 + 2z/R) \cdot (z/R)} - U_{\text{CPD}}. \quad (2)$$

The angle  $\theta$  is the angle of the dipole with respect to the surface normal.

As can be seen from equations (1) and (2), the Kelvin voltage  $U_{\text{dc},\text{min}}$  modulates around the CPD ( $U_{\text{CPD}}$ ) as a function of the sign and strength of the charge or dipole. For instance, a positive charge or dipole (positive end towards the surface) leads to a more positive Kelvin voltage, which agrees with the experimental findings. The voltage of +66 mV after tip-change V, where the tip became neutral, is the CPD ( $U_{\text{CPD}}$ ) between the tip and the surface. This value, which is close to zero, is reasonable because the tip was several times in contact with the surface before obtaining the images shown in figure 1—due to the contact with the surface, the tip probably became contaminated with the material of the surface like silver, leading to almost zero contact potential. Note that the work function of a tip, which changes its chemical composition by, for example, contamination, is no longer well defined. However, the observations described in this work are based on relative changes in the CPD, regardless of whether the work function of the neutral tip is well defined or not.

Tip-change-induced changes in the tip potential have so far been discussed only for positive and neutral. However, the mechanisms should also be valid for negative tips. Figure 3 shows a case where the tip changed from a positive tip to a neutral one and then to a negative tip. Similar

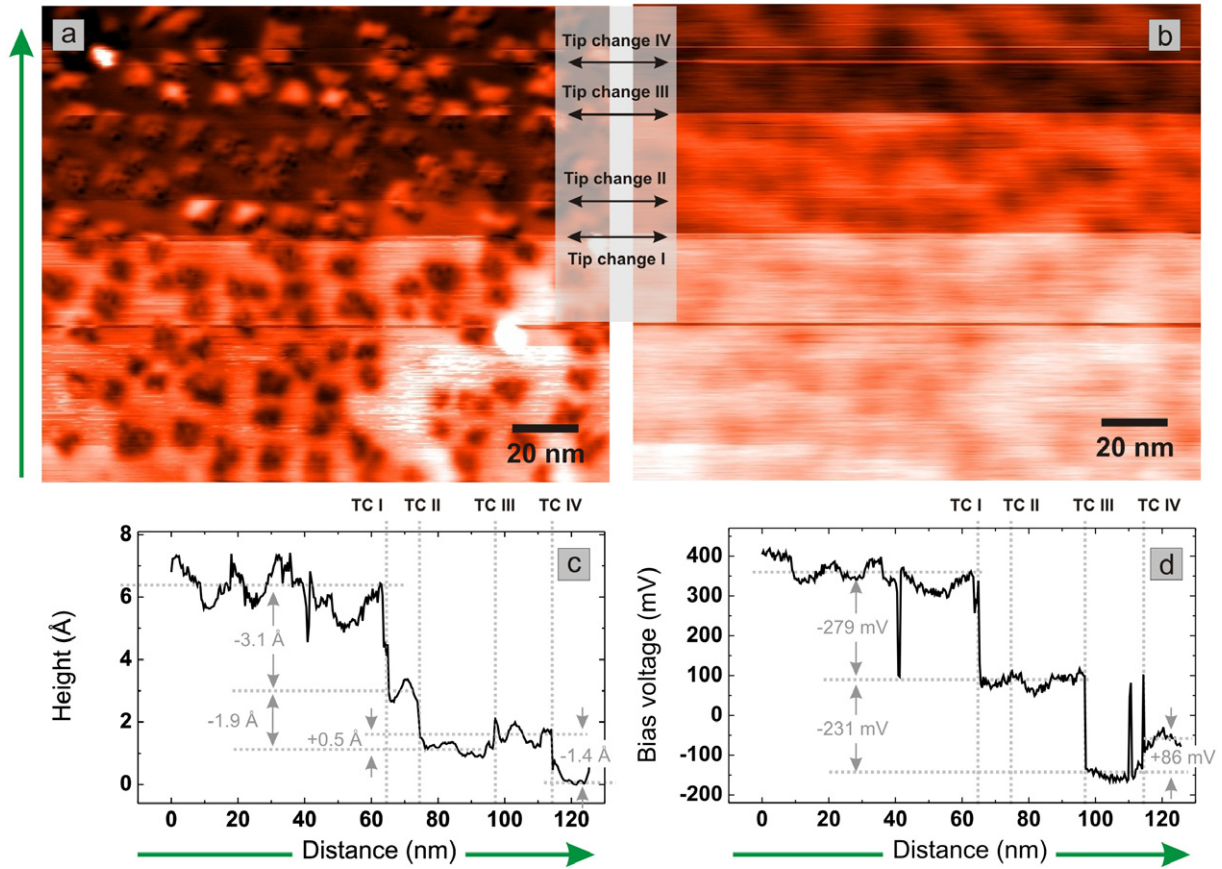


**Figure 3.** Raw topography (a) and Kelvin image (b) obtained within one measurement indicating the effect of a negatively charged tip. The tip-apex was probably smaller than the one in the measurement before (1), which explains that a lateral contrast of the MgO islands is visible in the Kelvin image (b). The slow scanning direction is shown on the left side of the topography image. (c, d) Averaged profiles along the slow scanning direction (green arrows). Contrast of the MgO islands:  $-4$  to  $-6$  Å (before TC I),  $+3.5$  to  $+7.8$  Å (TC I and TC II),  $\sim +2.5$  Å (TC II and TC III),  $+4.3$  to  $+8.7$  Å (TC III and TC IV).  $150 \times 126 \text{ nm}^2$ ,  $\Delta f = -30 \text{ Hz}$ ,  $v_{\text{Scan}} = 0.5 \text{ Hz}$ ,  $U_{\text{ac}} = 0.5 \text{ V}$  and  $f_{\text{ac}} = 630 \text{ Hz}$ .

to the measurement shown in figure 1(a), a positive tip imaged first the MgO islands as dark islands and changed its potential after tip-changes I and II to a neutral one imaging the MgO islands as bright islands with expected island heights. This interpretation is again consistent with the Kelvin signal, which decreased from  $+365 \text{ mV}$  to the CPD of  $+86 \text{ mV}$  (figures 3(b) and (d)). After tip-change III, the MgO islands appeared in a bright contrast with height values that are too large ( $4.5$ – $8.5$  Å for  $\text{MgO}_a$  and  $\text{MgO}_b$  islands) in comparison to the expected ones ( $h_{\text{MgO}-a} = 0.5$  Å and  $h_{\text{MgO}-b} = 2.4$  Å). This is a clear indication that the tip changed to a negative tip [18]. And, indeed, in complete agreement with this observation and the model, the Kelvin signal dropped from  $+86 \text{ mV}$  to  $-145 \text{ mV}$ . This value increased only slightly to  $-59 \text{ mV}$  after some slight tip-changes in the last scanning lines.

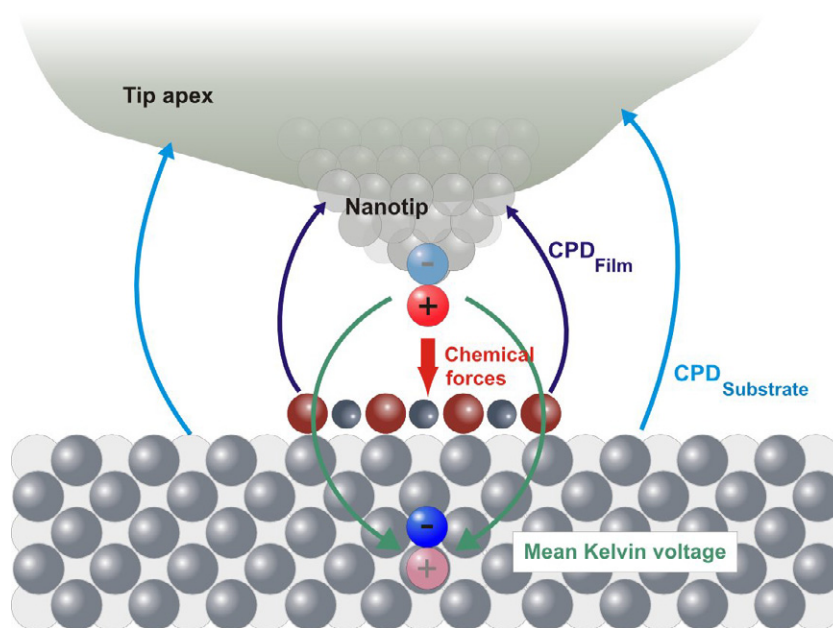


**Figure 4.** Contrast formation in nc-AFM and KPFM for tips that carry a charge or dipole at their apex and that are placed above a conducting surface covered by an MgO island. The charge or dipole at the tip contributes to the short-range chemical tip–surface interaction that is responsible for the topography contrast with high lateral resolution. At the same time, it polarizes the substrate (image charge/image dipole below the surface) and creates a long-range electrostatic tip–surface interaction, which is sensed by the mean Kelvin voltage. In contrast to the mean Kelvin voltage, the lateral Kelvin contrast depends on the polarization of the tip-apex by the island ( $\text{CPD}_{\text{Film}}$ ). Also, the silver surface in the periphery of the islands contributes to the lateral Kelvin contrast, if the tip apex is larger than the size of the island ( $\text{CPD}_{\text{Substrate}}$ ). The ion–ion distances in the island and atom–atom distances in the substrate are true-to-scale for the case of MgO on Ag(100).

Note that the lateral white to dark contrast in the Kelvin image (figure 3(b)) corresponds to a mean work function difference of  $-0.15$  to  $-0.3$  eV between MgO(001)/Ag(001) and Ag(001). This value is much smaller in comparison to the expected values of  $-1.0$  and  $-1.3$  eV for 1 and 2 ML thin MgO islands, respectively [18, 35]. Due to the long-range character of the electrostatic tip–surface interaction (figure 4), the lateral contrast of the Kelvin image is determined by the polarization of the complete tip-apex [18, 21, 36]. If the tip apex is smaller than the islands (blue arrows), the work function difference is well represented [18]. However, for a large tip-apex, the electrostatic interaction above the silver surface on the periphery of the MgO islands also contributes (bright blue arrows) so that a smaller work function difference is measured (see figure 3). In the first measurement (figure 1), the tip-apex was obviously so blunt that not even lateral resolution was obtained.

In fact, the polarization of the tip-apex by the MgO islands is opposite to the case above where it is the charged or polar tip, which polarizes a large part of the substrate via a long-range electrostatic interaction (green arrows). As will be discussed in the next section, single charged or polar species at the apex are sufficient to determine the electrostatic potential of charged or



polar tips. These species not only polarize the metal surface but also contribute to the short-range tip–surface interaction (red arrows), which determines the lateral contrast of topography images.

#### 4. Discussion

The topography contrast, which allows an assignment of the polarity of the tip, and the corresponding mean Kelvin voltage are correlated, indicating that KPFM is indeed sensitive to the tip potential: charged tips with a strong net negative or positive electrostatic potential can be distinguished from neutral tips, but also negative from positive tips. It is clear that ions, electrons and other charged species are responsible for the changes in the electrostatic tip potential that appear during the tip-changes. This raises fundamental questions: which and how many such species lead to a negative or positive tip potential, and can single quantities like single ions be detected by the Kelvin microscope?

The most probable material that can create positive or negative tips is the ionic magnesium oxide on the silver surface, which can indeed be picked up by the tip during contact with the surface [37]. Candidates for charges are, for example, ions of MgO (e.g.  $\text{Mg}^{2+}$  or  $\text{O}^{2-}$ ) [38],  $\text{F}^+$  or  $\text{F}^{++}$  centers [39],  $\text{O}_2^-$  ions [40] and even electrons [41], which are located at low-coordinated sites of the tip-apex and provide a sharp enough tip for the observed high lateral resolution in the topography images (figure 4). These species can, in principle, also form dipoles—in the simplest case an MgO molecule adsorbed at a low-coordinated site at the tip apex. More complicated tip structures can be built from non-stoichiometric MgO clusters [18, 38, 42], where charged species are trapped at its very end [38]. Molecules from the residual gas of the UHV that have a permanent dipole like water or  $\text{OH}^-$  could also adsorb at the tip. However, they are not expected to play a large role because the adsorption probability is relatively low in UHV on the timescale where tip-changes appear during scanning.

In figure 5, the distance-dependent Kelvin voltage is shown for a representative cation (red curve) and dipole (blue curve) at the tip (tip radius = 5 nm). The two curves were calculated by using equations (1) and (2) for an ion and a dipole with a strength of  $q \delta = 1.8 e \text{ \AA}$  and  $p \cos(0^\circ) = 14.3$  Debye, respectively. The curves mimic an  $\text{Mg}^+$  ion at a distance of  $1.8 \text{ \AA}$  from the tip and a polarized MgO molecule at the tip (see supporting information). In addition, the results obtained from atomistic calculations for the same  $\text{Mg}^+$  ion and MgO molecule are shown, as well as for a mixed charge/dipole tip (light gray) and a stoichiometric MgO tip (dark gray) (see supporting information). As can be seen, the simplified models are in excellent agreement with their equivalent atomistic models. The curves show that the cation (red curve) and polar molecule (blue curve) strongly polarize the metal substrate at tip–surface distances smaller than 1 nm. At a distance of 1 nm, the Kelvin voltage is  $\sim 200$  mV (charge) and 400 mV (dipole). At distances between 1 and 3 nm, which are typical distances in nc-AFM and KPFM, the Kelvin voltage is in the range of 200–80 mV for the charge and between 300 and 150 mV for the dipole. In contrast to the polar tips, the mixed and stoichiometric tips yield only small Kelvin voltages of a few tens of mV. Note that the Kelvin voltage decreases as the tip radius increases (see supporting information). For a tip radius of 20 nm and within a distance range between 1 and 3 nm to the surface, Kelvin voltages between 80 and 20 mV (charge) and 100 and 30 mV (dipole) can be found.

In the light of the quantification given by the model, the mean topography and Kelvin signals from the experiments can now be analyzed in order to characterize the imaging species

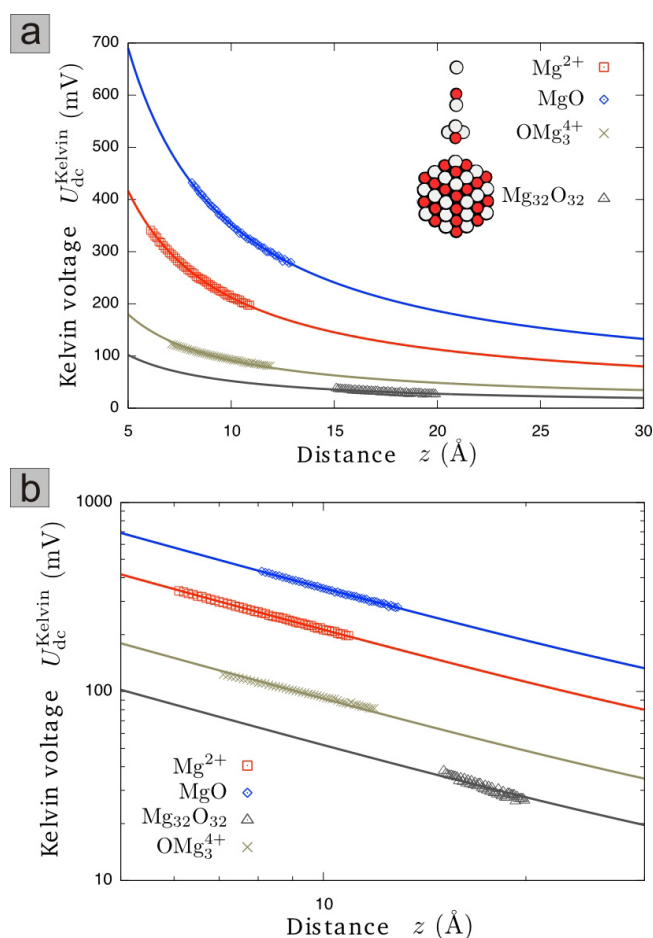


**Figure 5.** Distance-dependent mean Kelvin voltage, with (a) a linear and (b) a log–log scale, for an ion ( $\text{Mg}^+$  with  $q\delta = 1.8 \text{ e}\text{\AA}$ , red curve), a dipole ( $\text{MgO}$  molecule with  $p = 14.3$  Debye, blue curve), a mixed charge/dipole cluster (light gray curve) and a stoichiometric  $\text{Mg}_{32}\text{O}_{32}$  cluster (dark gray curve) at the tip with radius  $R = 5 \text{ nm}$ . The straight curves were obtained by using equations (1) and (2). The data points are from atomistic calculations (see supporting information). For simplicity, the CPD between the tip and the surface was set to zero ( $U_{\text{CPD}} = 0$ ).

at the tip. As can be seen in the topography profiles in figures 1(c) and 3(c), the mean surface plane changed upon most of the tip-changes, indicating changes in the tip length. This means that either the tip atoms changed their adsorption site at the tip apex or material was exchanged between the tip and the surface. If the latter is assumed, the tip obviously lost material from its apex in the two measurements in figures 1 and 3. The changes in the tip length are mostly in the angstrom range and rarely reach values of more than 1 nm. This suggests that single atomic species are responsible for the change in the tip length. At the same time, when a tip-change appears, the mean Kelvin signal changes, which demonstrates that these species also influence the mean Kelvin contrast. This is in perfect agreement with the calculations shown in figure 5, which mimic the interaction of a single ion and dipole at the tip and where values are quite similar to the experimental ones for positive and negative tips. It can therefore be concluded

that the changes observed in the mean Kelvin voltage indeed belong to single ions or dipoles of atomic size at the tip-apex.

Note that if several positive or negative ions or dipoles are considered, the Kelvin voltage would reach much larger values, which is in disagreement with the experimental values. This is not surprising because a tip apex carrying many repelling charges would be unstable. However, this does not necessarily mean that a few charged species at the tip cannot indeed coexist and contribute to the topography and mean Kelvin contrast. The lateral resolution of the topography image (a) in figure 1 is about 1 nm or less, which suggests that a single ion or dipole at a very blunt tip-apex was the imaging element of the tip. In comparison, the topography image (a) of figure 3 has a much lower lateral contrast. If the mean Kelvin voltages of both measurements are compared, the mean Kelvin voltage for the positive tip in the second measurement is larger than the one of the first measurement (compare figure 3(d) with figure 1(d)). The somewhat lower topography contrast but larger mean Kelvin voltage in the second measurement (3) can be tentatively assigned to an increased number of similarly charged species at the tip (e.g. two instead of one). The analysis shows furthermore how single charges or dipoles rearrange at the tip or are picked up from the surface or desorbed from the tip during tip-changes: amazingly, the changes in the Kelvin voltage are discrete. In the first measurement (figure 1(d)), a change in the Kelvin voltage always measures 80–90 mV, whereas in the second measurement (figure 3(d)), a change in the Kelvin signal always corresponds to roughly 230 mV. It can be speculated that these discrete changes in the mean Kelvin voltage are due to single ions, which get attached to or detached from the tip. Values in between do not appear because the charge of a single ion is already a discrete quantity.

## 5. Conclusion and perspectives

In this paper, it is shown that single charged species, such as ions or dipoles, at the tip-apex modulate the CPD between the tip and the surface, producing a shift of up to 100 mV or more in the mean Kelvin voltage. Thanks to the directionality of the electrostatic field between the tip and the surface, the tip can be identified as a negative, positive or neutral tip with the help of the mean Kelvin signal. The dependence of the mean Kelvin signal on charges or dipoles at the tip is consistently proven by nc-AFM and KPFM measurements on a dipolar interface, namely thin MgO(001) islands grown on Ag(001), where the symmetry of the electrostatic tip–surface interaction is broken by the interfacial dipole moment of the islands. Theoretical models support the picture that single ions or dipoles indeed produce a Kelvin voltage in the 10–100 mV range. All this is not restricted to conducting surfaces but is applicable also to the surfaces of insulators, which can be equally polarized in the presence of charges or dipoles [43].

The mean Kelvin voltage is thus the critical parameter that unequivocally characterizes the charge state of the tip, which is useful for any type of experiment. An obvious application of a *Kelvin identified tip* (KIT) is certainly atomic resolution imaging of ionic surfaces, where the electrostatic potential of the last imaging ion or dipole strongly determines the atomic image contrast [44]. The same holds for ions, polar molecules and charged nanoclusters, which are supported on the surface. The characterization of atomic or molecular species with the help of a KIT becomes a complete experimental procedure, when the tip is intentionally functionalized by picking up known ions or polar molecules from the surface [29, 45].

Furthermore, charged or polar tips always play a role when charges are transferred between the tip and the surface [46]. In such charging experiments where the tip and the surface are not in

contact with each other, metal clusters or carbon nanotubes on surfaces [47] and also nanodots at the tip [48] can be charged, in principle. The mean Kelvin signal can then be used to determine the transferred charge before, during and after such types of experiments or even as a function of time.

The approach opens new doors to the exploration of even more complex systems, such as molecular systems [10, 49] or even proteins in biology [50], where KITs can be used for the characterization of structure and electrostatics and for controlled manipulation experiments by charge injection.

## Acknowledgments

This work was supported by the European COST program through Action D41 and by the European Science Foundation through the FANAS project NOMCIS. UH also acknowledges support from the DFG and HBF. We acknowledge stimulating discussions with AL Shluger and E Bussmann.

## References

- [1] Kelvin L, Fitzgerald G and Francis W 1898 Contact electricity of metals *Phil. Mag.* **46** 82
- [2] Zisman W A 1932 A new method of measuring contact potential differences in metals *Rev. Sci. Instrum.* **3** 367
- [3] Schroder D K 2001 Surface voltage and surface photovoltage: history, theory and applications *Meas. Sci. Technol.* **12** R16
- [4] Christmann K, Ertl G and Pignet T 1976 Adsorption of hydrogen on a Pt(111) surface *Surf. Sci.* **54** 365
- [5] Ertl G, Neumann M and Streit K M 1977 Chemisorption of CO on the Pt(111) surface *Surf. Sci.* **64** 393
- [6] Binnig G, Quate C F and Gerber Ch 1986 Atomic force microscope *Phys. Rev. Lett.* **56** 930
- [7] Girard P 2001 Electrostatic force microscopy: principles and some applications to semiconductors *Nanotechnology* **12** 485
- [8] Nonnenmacher M, Boyle O M P and Wickramasinghe H K 1991 Kelvin probe force microscopy *Appl. Phys. Lett.* **58** 2921
- [9] Weaver J M R and Abraham D W 1991 High resolution atomic force microscopy potentiometry *J. Vac. Sci. Technol. B* **9** 1559
- [10] Palermo V, Palma M and Samori P 2006 Electronic characterization of organic thin films by Kelvin probe force microscopy *Adv. Mater.* **18** 145
- [11] Berger R, Butt H J, Retschke M B and Weber S A L 2009 Electrical modes in scanning probe microscopy *Macromol. Rapid Commun.* **30** 145
- [12] Morita S, Wiesendanger R and Meyer E 2002 *Noncontact Atomic Force Microscopy* (Berlin: Springer)
- [13] Kikukawa A, Hosaka S and Imura R 1996 Vacuum compatible high-sensitive Kelvin probe force microscopy *Rev. Sci. Instrum.* **67** 1463
- [14] Kitamura S and Iwatsuki M 1998 High-resolution imaging of contact potential difference with ultrahigh vacuum noncontact atomic force microscope *Appl. Phys. Lett.* **72** 3154
- [15] Sommerhalter C, Matthes T W, Glatzel T, Jäger-Waldau A and Lux-Steiner M C 1999 High-sensitivity quantitative Kelvin probe microscopy by noncontact ultra-high-vacuum atomic force microscopy *Appl. Phys. Lett.* **75** 286
- [16] Krok F, Kolodziej J J, Such B, Czuba P, Struski P, Piatkowski P and Szymonski M 2004 Dynamic force microscopy and Kelvin probe force microscopy of KBr film on InSb (0 0 1) surface at submonolayer coverage *Surf. Sci.* **566** 63



- [17] Loppacher C, Zerweck U and Eng L M 2004 Kelvin probe force microscopy of alkali chloride thin films on Au *Nanotechnology* **15** 9
- [18] Bielecki M, Hynninen T, Soini T M, Pivetta M, Foster A S, Esch F, Barth C and Heiz U 2010 Topography and work function measurements of thin MgO(001) films on Ag(001) by nc-AFM and KPFM *Phys. Chem. Chem. Phys.* **12** 3203
- [19] Goryl M, Krok F, Kolodziej J J, Piatkowski P, Such B and Szymonski M 2004 Surface structure of Au/InSb (001) system investigated with scanning force microscopy *Vacuum* **74** 223
- [20] Zerweck U, Loppacher C, Otto T, Grafström S and Eng L M 2007 Kelvin probe force microscopy of C60 on metal substrates: towards molecular resolution *Nanotechnology* **18** 84006
- [21] Glatzel T, Zimmerli L, Koch S, Such B, Kawai S and Meyer E 2009 Determination of effective tip geometries in Kelvin probe force microscopy on thin insulating films on metals *Nanotechnology* **20** 264016
- [22] Enevoldsen G H, Glatzel T, Christensen M C, Lauritsen J V and Besenbacher F 2008 Atomic scale Kelvin probe force microscopy studies of the surface potential variations on the TiO<sub>2</sub>(110) surface *Phys. Rev. Lett.* **100** 236104
- [23] Barth C and Henry C R 2006 Kelvin probe force microscopy on surfaces of UHV cleaved ionic crystals *Nanotechnology* **17** S155
- [24] Barth C and Henry C R 2007 Surface double layer on (001) surfaces of alkali halide crystals: a scanning force microscopy study *Phys. Rev. Lett.* **98** 136804
- [25] Barth C and Henry C R 2006 Gold nanoclusters on alkali halide surfaces: charging and tunneling *Appl. Phys. Lett.* **89** 252119
- [26] Barth C and Henry C R 2009 Kelvin probe force microscopy on MgO (001) surfaces and supported Pd nanoclusters *J. Phys. Chem. C* **113** 247
- [27] Terris B D, Stern J E, Rugar D and Mamin H J 1989 Contact electrification using force microscopy *Phys. Rev. Lett.* **63** 2669
- [28] Busmann E B, Zheng N and Williams C C 2006 Imaging of localized electronic states at a nonconducting surface by single-electron tunneling force microscopy *Nano Lett.* **6** 2577
- [29] Gross L, Mohn F, Moll N, Liljeroth P and Meyer G 2009 The chemical structure of a molecule resolved by atomic force microscopy *Science* **325** 1110
- [30] Bohmisch M, Burmeister F, Rettenberger A, Zimmermann J, Boneberg J and Leiderer P 1997 Atomic force microscope based Kelvin probe measurements: application to an electrochemical reaction *J. Phys. Chem. B* **101** 10162
- [31] Kantorovich L N, Livshits A I and Stoneham M 2000 Electrostatic energy calculation for the interpretation of scanning probe microscopy experiments *J. Phys. Cond. Mater.* **12** 795
- [32] Kantorovich L N, Foster A S, Shluger A L and Stoneham A M 2000 Role of image forces in NC-SFM images of ionic surfaces *Surf. Sci.* **445** 283
- [33] Valeri S, Altieri S, Del Pennino U, Di Bona A, Luches P and Rota A 2002 Scanning tunnelling microscopy of MgO ultrathin films on Ag (001) *Phys. Rev. B* **65** 245410
- [34] Ferrari A M, Casassa S and Pisani C 2005 Electronic structure and morphology of MgO submonolayers at the Ag (001) surface: an *ab initio* model study *Phys. Rev. B* **71** 155404
- [35] Prada S, Martinez U and Pacchioni G 2008 Work function changes induced by deposition of ultrathin dielectric films on metals: a theoretical analysis *Phys. Rev. B* **78** 235423
- [36] Krok F, Sajewicz K, Konior J, Goryl M, Piatkowski P and Szymonski M 2008 Lateral resolution and potential sensitivity in Kelvin probe force microscopy: Towards understanding of the sub-nanometer resolution *Phys. Rev. B* **77** 235427
- [37] Livshits A I and Shluger A L 1997 Self-lubrication in scanning-force-microscope image formation on ionic surfaces *Phys. Rev. B* **56** 12482
- [38] Aguado A, López-Gejo F and López J M 1999 Structures and stabilities of doubly charged (MgO) Mg ( $n = 1-29$ ) cluster ions *J. Chem. Phys.* **110** 4788

- [39] Kantorovich L N, Holender J M and Gillan M J 1995 The energetics and electronic structure of defective and irregular surfaces on MgO *Surf. Sci.* **343** 221
- [40] Ricci D, Pacchioni G, Sushko P V and Shluger A L 2003 Reactivity of  $(\text{H}^+)(\text{e}^-)$  color centers at the MgO surface: formation of  $\text{O}_2^-$  and  $\text{N}_2^-$  radical anions *Surf. Sci.* **542** 293
- [41] Ricci D, Pacchioni G, Sushko P V and Shluger A L 2002 Electron trapping at neutral divacancy sites on the MgO surface *J. Chem. Phys.* **117** 2844
- [42] Recio J M and Pandey R 1993 *Ab initio* study of neutral and ionized microclusters of MgO *Phys. Rev. A* **47** 2075
- [43] Jackson J D 1999 *Classical Electrodynamics* (Berlin: Wiley)
- [44] Hofer W A, Foster A S and Shluger A L 2003 Theories of scanning probe microscopes at the atomic scale *Rev. Mod. Phys.* **75** 1287
- [45] Eigler D M, Lutz C P and Rudge W E 1991 Atomic switch realised with the scanning tunnelling microscope *Nature* **352** 600
- [46] Schönenberger C and Alvarado S F 1990 Observation of single charge carriers by force microscopy *Phys. Rev. Lett.* **65** 3162
- [47] Zdrojek M, Melin T, Boyaval C, Stievenard D, Jouault B, Wozniak M, Huczko A, Gebicki W and Adamowicz L 2005 Charging and emission effects of multiwalled carbon nanotubes probed by electric force microscopy *Appl. Phys. Lett.* **86** 213114
- [48] Klein L J, Williams C C and Kim J 2000 Electron tunneling detected by electrostatic force *Appl. Phys. Lett.* **77** 3615
- [49] Hallam T, Lee M, Zhao N, Nandhakumar I, Kemerink M, Heeney M, McCulloch I and Sirringhaus H 2009 Local charge trapping in conjugated polymers resolved by scanning Kelvin probe microscopy *Phys. Rev. Lett.* **103** 256803
- [50] Sinensky A and Belcher A 2007 Label-free and high-resolution protein/DNA nanoarray analysis using Kelvin probe force microscopy *Nat. Nanotechnol.* **2** 653